Hindawi Publishing Corporation
Advances in Chemistry
Volume 2014, Article ID 301410, 7 pages
http://dx.doi.org/10.1155/2014/301410

Research Article

Effect of γ-Irradiation and Calcination Temperature of Nanosized ZnO/TiO_2 System on Its Structural and Electrical Properties

Abdelrahman A. Badawy,[1] Shaymaa E. El-Shafey,[2] Suzan Abd El All,[3] and Gamil A. El-Shobaky[2]

[1] *Physical Chemistry Department, Center of Excellence for Advanced Science, Renewable Energy Group, National Research Center, Dokki, Cairo 12622, Egypt*
[2] *Physical Chemistry Department, National Research Center, Dokki, Cairo 12622, Egypt*
[3] *Radiation Physics Department, National Center for Radiation Research and Technology (NCRRT), Nasr City, Cairo 11762, Egypt*

Correspondence should be addressed to Abdelrahman A. Badawy; aabadawy107@yahoo.com

Received 2 May 2014; Revised 3 June 2014; Accepted 13 June 2014; Published 18 August 2014

Academic Editor: Fabien Grasset

ZnO/TiO_2 powders were synthesized by sol-gel method using ammonium hydroxide. The effects of calcination temperature (500–1000°C) and gamma rays (with doses from 25 to 150 kGy) on the phases present and their electrical properties were investigated. The results revealed that heating the system investigated at 500°C led to the formation of $ZnTiO_3$-rohom and TiO_2-rutile. The degree of crystallinity of the phases produced increased by increasing the calcination temperature. When heating at 1000°C, $ZnTiO_3$-rohom turned to $ZnTiO_3$-cubic but the rutile phase remained stable. γ-Irradiation decreased considerably the crystallite size of the rutile phase from 146 to 63 nm and that of $ZnTiO_3$-cubic decreased from 101 to 39 nm. This treatment led also to the creation of holes in the matrix of irradiated solids which increased the mobility of charge carriers (electrons) leading to a significant increase in the electrical conductivity reaching to 10^2 to 10^3-fold.

1. Introduction

Fundamental studies concerning the phase diagram and characterization of ZnO-TiO_2system have been published since 1960s. This system still attracts the attention of researchers because of its importance in practical applications [1–5]. TiO_2 ceramics have been investigated for diverse applications in the optical and semiconductors industries because of their interesting semiconducting and dielectric properties. Semiconducting titania had especially been employed in producing different electronic devices, including oxygen sensors, varistors, and current collecting electrodes in Na-S batteries [6–8]. TiO_2-ZnO-based compounds have been employed as promising catalysts in some chemical industries. Many attempts have been made to improve the photoelectrochemical (PEC) conversion efficiency of TiO_2 ceramics by treatment with certain compounds including Al_2O_3[9–14] and BeO [15]. The base of the phase diagram for this system was established by Dulin and Rase [1], who have reported that there are three compounds existing in the ZnO-TiO_2 system, including Zn_2TiO_4 (cubic), $ZnTiO_3$ perovskite metatitanate (hexagonal), and $Zn_2Ti_3O_8$ (cubic) [16]. $ZnTiO_3$ has perovskite structure and could be considered as a useful candidate for microwave resonator materials [17] and gas sensor [18] and as a catalyst for oxidation of ethanol NO, CO, and so forth . . ., [2] and colour pigments [11]. Yamaguchi et al. [3] claimed that Zn_2TiO_4 can be easily prepared by conventional solid-state reaction between 2 moles of ZnO and 1 mole of TiO_2. However, preparation of pure $ZnTiO_3$ from a mixture of equimolar proportion of zinc and titanium oxides has not been successful because the produced compound undergoes partial decomposition by heating at 900°C into a mixture of ZnO and rutile.

It is well known that the properties of materials depend on their synthesis processes and calcination conditions. For $ZnTiO_3$, its physicochemical properties are influenced by their preparation conditions. In general, there are some methods to prepare $ZnTiO_3$ powder, including conventional solid-state reaction [1], sol-gel method [19], . . ., and so forth. The solid-state reaction method has some drawbacks including high temperature, large particle size, and limited degree of chemical homogeneity. The chemical solution methods can provide products of fine and homogeneous particles with high specific surface area. The processing of complex oxide ceramics using sol-gel techniques has been extensively studied [20–23]. The Pechini method is a conventional approach to prepare powder consisting of oxides of transition metals. This method requires first dissolution of hydrous oxides or alkoxides of element in polyhydroxy alcohol such as ethylene glycol, with a chelating agent, such as citric acid. Subsequently thermal treatment is performed at relatively low temperatures leading to the formation of highly homogenous powder [24].

In addition, much attention has been paid to their electrical properties leading to numerous applications as solid oxides fuel cells (SOFCs) [25]. Some progress of microwave devices in the area of mobile telephones and satellite communications brought the need for development of microwave dielectrics with low dielectric loss, high dielectric constant, and low-temperatures coefficient of resonant frequencies. It has been demonstrated that zinc titanates are good dielectric materials for microwave devices [26–29]. So, they are nowadays widely applied as dielectric resonators and filters [25].

Damage of solids caused by ionizing radiations occurs mostly below the surface of the material and often creates features very small in size (nm to μm in scale). The characteristics of the damage can be either microstructure (dislocation loops, voids, and structural disordering) or microchemical (segregation) or both (precipitation of secondary phase) [30]. In certain materials a permanent change in their electrical conductivity may be induced by radiation damage of the crystal.

In this paper, the authors have attempted to prepare $ZnTiO_3/TiO_2$ composite ceramic materials by sol-gel method. The role of calcination temperature and exposure to different doses of γ-rays of the obtained solids on their structural and electrical properties were investigated. The techniques employed were DTA, XRD, SEM, and electrical conductivity.

2. Experimental Details

2.1. Materials. TiO_2/ZnO mixed solids were prepared using the following method: certain amounts of $ZnClO_4$ and $TiClO_4$ with stoichiometry (Zn/Ti = 1 : 1) were dissolved in distilled water stirred for 3 hours. NH_4OH solution was added dropwise to mixed solutions as a precipitating agent. The precipitation process was carried out at room temperature and a pH of about 8. The precipitate was dried at 70°C for two days and the large agglomerates were pulverized in an agate mortar. The ceramic composite was obtained after heating in air for 6 hours at temperatures between 500 and 1000°C. Systematic studies concerning the role of calcination temperature and doses of gamma rays on structural and electric properties of the treated solids were investigated.

The irradiation process was performed in air, at room temperature, where a cooling system was used in the irradiation chamber to avoid heating of the samples during irradiation. The irradiated solids were kept in sealed tubes for 3 weeks before carrying out any measurements. The doses of γ-rays were 25, 50, 100, and 150 kGy.

2.2. Techniques. X-ray powder diffractograms of nonirradiated and variously irradiated samples calcined at temperatures within 500 and 1000°C were obtained using a Bruker diffractometer (Bruker D8 advance target). The patterns were run with Cu Kα1 with secondly monochromator (λ = 1.5405 Å) at 40 kV and 40 mA. The crystallite size of crystalline phases present in different solids investigated was calculated from line broadening profile analysis of the main diffraction lines of crystalline phases present using the Scherer equation [18]:

$$d = \frac{K\lambda}{\beta_{1/2}} \cos\theta, \tag{1}$$

where d is the mean crystallite diameter, λ is the wave length of X-ray beam, K is the Scherer constant (0.89), $\beta_{1/2}$ is full width at half maximum {FWHM} of the main diffraction peaks in radians, and θ is the diffraction angle. The scanning rate was 8° and 0.8° in 2θ/min in phase identification and line broadening profile analysis, respectively.

Differential thermal analysis (DTA) measurements were carried out by Shimadzu instrument (DTA-50) calibrated through the melting points of indium and tin. The thermogravimetric analysis (TGA) was recorded using the (TGA-50) system in the presence of air, within a temperature range from room temperature up to 600°C at a heating rate of 30°C min^{-1}. The nature and morphological feature of composite ceramic were studied by scanning electron microscope SEM (JOEL, JSM).

The electrical conductivity measurements were performed using a locally designed electrical circuit, where the samples were pressed under hydraulic pressure of 9 ton cm^{-2} in the form of discs of a cross-sectional area of 0.6129 cm^2. A Tennelec TC 952 power supply was used to apply DC voltage across the sample discs, and the resulting current was measured using a digital electrometer (Model 6517A, manufactured by Keithely, USA).

3. Results and Discussion

3.1. Thermal Behavior of Composite Powders. It is well know that the sol-gel technique has the unique advantage of providing extremely small and uniform particle size for the precursor powders. The prepared powders were analyzed using DTA-TGA for burnout behaviors.

Figure 1 shows TG-DTA curves of the prepared noncalcined mixed solids, being dried at 70°C and having equimolar ratio of ZnO and TiO_2 existing as an amorphous powder. The DTA curve shows an endothermic reaction at ~200°C, which

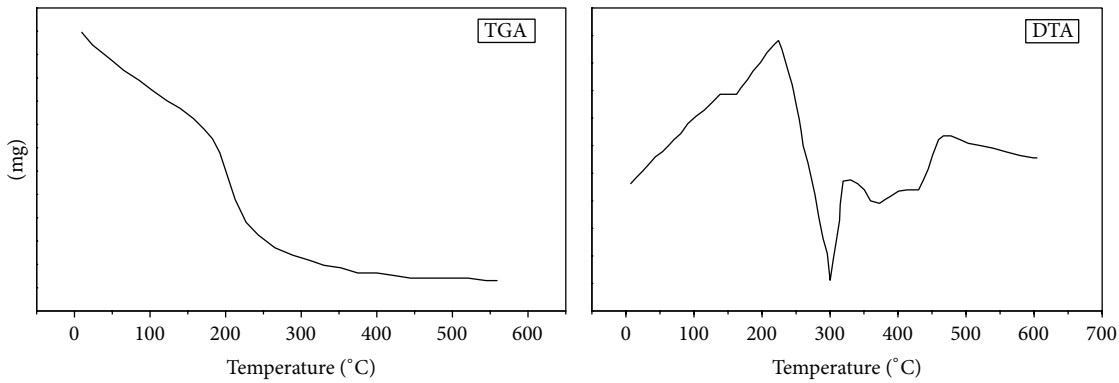

Figure 1: TGA-DTA curves of ZnO/TiO_2 systems.

is attributed to the loss of the remaining absorbed water as shown in Figure 1. This finding agrees with the weight loss given by TGA data as shown in Figure 1, an endothermic peak at above 200°C could be attributed to the formation of TiO_2/ZnO particles. A broad endothermic peak due to the crystallization of TiO_2/ZnO is observed at about 470°C, resulting from the dehydroxylation of titanium and zinc hydroxides into TiO_2 and ZnO phases, respectively.

3.2. XRD Investigation of ZnO/TiO_2 System Calcined at Different Temperatures. X-ray diffractograms of ZnO/TiO_2 system calcined at 500, 600, 800, and 1000°C were determined. Figure 2 shows the recorded diffractograms. Examination of Figure 2 shows the following: (i) the mixed solids calcined at 500, 600, and 800°C consisted of TiO_2-rutile as a major phase together with $ZnTiO_3$-rohom. The absence of any diffraction line of ZnO phase in different solids investigated calcined at 500–1000°C might suggest its possible presence in dissolved form in TiO_2 lattice forming solid solution. The dissolution of ZnO in TiO_2 lattice stabilized the rutile structure playing almost the role of Al_2O_3 dissolved in TiO_2[9]. This conclusion is reached by phase transformation of TiO_2 from rutile to anatase by heating a temperature below 1000°C. (ii) The increase in the calcination temperature within 500–1000°C brought about an effective increase in the degree of crystallinity of the phases present. (iii) Increasing the calcination temperature of the system investigated up to 1000°C led to a phase transition process of $ZnTiO_3$-rohom into cubic $ZnTiO_3$ structure. (iv) The average crystallite size of TiO_2-rutile in solids calcined at 500–1000°C was calculated from the Scherrer equation [18]. The computed values of crystallite size of TiO_2-rutile in mixed solids calcined at 500, 600, 800, and 1000°C measured 63, 74, 82, and 146 nm, respectively. (vi) The crystallite size of the $ZnTiO_3$-rohom in mixed solids calcined as 500, 600, and 800°C measured 83, 78, and 74 nm, respectively while the crystallite size of $ZnTiO_3$-cubic present in mixed solid calcined at 1000°C reached 101 nm. These results show clearly an effective sintering of the rutile phase due to increasing its calcination temperature within 500–1000°C.

3.3. Effect of Gamma Radiation on Structural Characteristics of ZnO/TiO_2 System. ZnO/TiO_2 samples calcined at 1000°C and exposed to γ-rays with absorbed doses from 25 to 150 kGy were analyzed by XRD technique. The recorded diffractograms are illustrated in Figure 3. It is clear from this figure that γ-rays did not induce any change in the present crystalline phases. The crystallite size of detected phases (TiO_2-rutile and Zn TiO_3) was measured from XRD data applying the Scherrer equation [19–29]. The computed values of the crystallite size of rutile phase were found to be equal to 146, 63, 100, and 102 nm for nonirradiated sample and those exposed to 25, 50, 100, and 150, respectively. These values show clearly that γ-irradiation induced progressive decreasing of the crystallite size of rutile phase. The lower value of this latter was observed at 50 kGy. The decrease in the crystallite size reached about 57% in case of $ZnTiO_3$-cubic formed by heating ZnO/TiO_2 at 1000°C. Its crystallite size measured 101 nm and decreased considerably after irradiation at 25, 50, 100, and 150 kGy to reach 63, 51, 49, and 39 nm, respectively. Similar results have been reported in case of Co_3O_4/Al_2O_3 system calcined at 650°C [30] by exposure to γ-rays with high doses (50 MGy). After irradiation, the crystallite size of Co_3O_4 decreased effectively via splitting its crystallites to an extent proportional to the absorbed dose. It fell to a minimum value and the increased with the dose upon 50 MGy. Such a very high dose might increase the degree of aggregation of small-sized particles.

3.4. SEM Micrographs of the Powder. Figure 4 shows SEM pictures realized for a nonirradiated sample of ZnO/TiO_2 and samples irradiated at doses of 25, 50, 100, and 150 kGy. These pictures revealed that, before irradiation and at relatively low doses, there were few small black holes dispersed in the whole mass of the samples. It appears from Figure 4 that the concentration of these holes increased by increasing the dose. These created holes or cavities in the irradiated solids might reflect an order-disorder transition from the cation and not to a phase shift or due to charged oxygen vacancies, which are systematically generated by irradiation in the oxides. These created holes or cavities are expected to increase

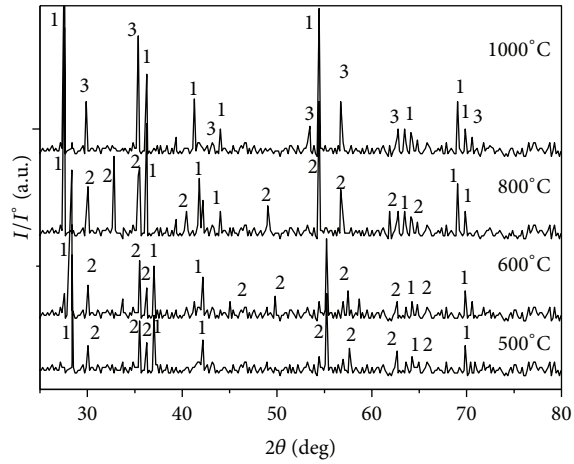

Figure 2: XRD diffractograms of ZnO_2/TiO_2 powders calcined at temperatures of 500–1000°C. 1 → TiO_2-rutile, 2 → $ZnTiO_3$(R), 3 → $ZnTiO_3$ (c).

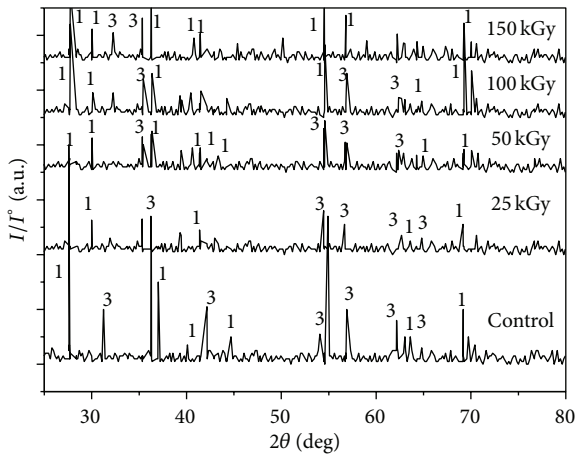

Figure 3: XRD diffractograms of effect of γ ray on the ZnO/TiO_2 solids calcined at 1000°C. 1 → TiO_2 (rutile), 3 → $ZnTiO_3$ (c).

the electrical conductivity of the irradiated solids via increasing the mobility of charge carriers.

3.5. Effect of Calcination Temperature of ZnO/TiO_2 System on Its Electrical Properties. The electrical conductivity (σ) of ZnO/TiO_2 system calcined at temperature within 500–1000°C was investigated. It was measured for various solids at temperatures between 25 and 150°C. Figure 5(a) shows log σ as a function of $1/T$ for variously calcined solids. It appears that these solids behave as a semiconductor. In fact, one can observe that the conductivity exhibits Arrhenius behavior, which can be expressed as

$$\sigma = \sigma_0 \exp\left(-\frac{\Delta E}{kT}\right), \tag{2}$$

where σ is the electrical conductivity at a given absolute temperature T, σ_0 is the preexponential factor of the Arrhenius equation, ΔE is the activation energy of electric conductivity of the sample under test, and k is the Boltzmann constant. From this relation the activation energy can be calculated and the results obtained are illustrated in Figure 5(b).

As both TiO_2 and ZnO are known to show n-type semiconducting character, the variation of conductivity can be influenced by the change in concentration and mobility of charge carriers (electrons) induced by the possible defect reactions. Furthermore, it has been reported that because TiO_2 contains interstitial channels in the c direction, certain transition metal cations diffuse through these channels into lattices. The diffused cations are located preferentially in interstitial and/or in host cation positions via substituting some of the host lattice cations [31]. Thus, the decrease of conductivity with increasing the sintering temperature, despite the increase in crystallite size, can be explained by substitution of Zn^{+2} (0.74 Å) by Ti^{+4} (0.68 Å) with subsequent decrease in the concentration of electrons.

It is seen from Figure 5(a) that σ, measured at different temperatures, decreases progressively as a function of calcination temperature of the system investigated. A higher calcination temperature increased the degree of crystallinity of the phases present as shown in XRD Section 3.2. The observed increase in the degree of crystallinity of the phases present may act as an energy barrier opposing the flow of the electric current leading to a decrease in σ value with subsequent increase in the activation energy. The decrease in σ value due to increasing the calcination temperature might also result from occupation of cationic vacancies by which decreases the diffusion of oxygen anions [10].

In certain materials a permanent change in electrical conductivity may take place as a result of a possible induced damage due to exposure to ionizing radiations.

3.6. Effect of γ Irradiation on Electrical Properties of ZnO/TiO_2 System Calcined at 1000°C. The electrical conductivity of ZnO/TiO_2 sample calcined at 1000°C and exposed to γ-rays with different absorbed doses was measured at temperatures between 25 and 150°C. The results obtained are graphically illustrated in Figure 6(a). It is clearly shown from this figure that σ increases progressively as a function of the absorbed dose of γ-rays. This increase in σ value attained 10^2-10^3-fold. The change in the activation energy of electric conductivity (ΔE_σ) as a function of the absorbed dose of γ-rays was calculated and the results obtained are given in Figure 6(b). The measurable increase in σ value and the subsequent decrease in (ΔE_σ) might be attributed to possible lattice defects via displacing of atoms from their equilibrium position together with creation of an increased number of holes throughout the whole mass of the irradiated solids (c.f. Figure 4). The produced holes facilitate diffusion of charge carriers across the matrices of the irradiated solids resulting in an effective increase in the electrical conductivity with subsequent decrease in (ΔE_σ).

4. Conclusions

The following are the main conclusions that may be drawn from the results obtained.

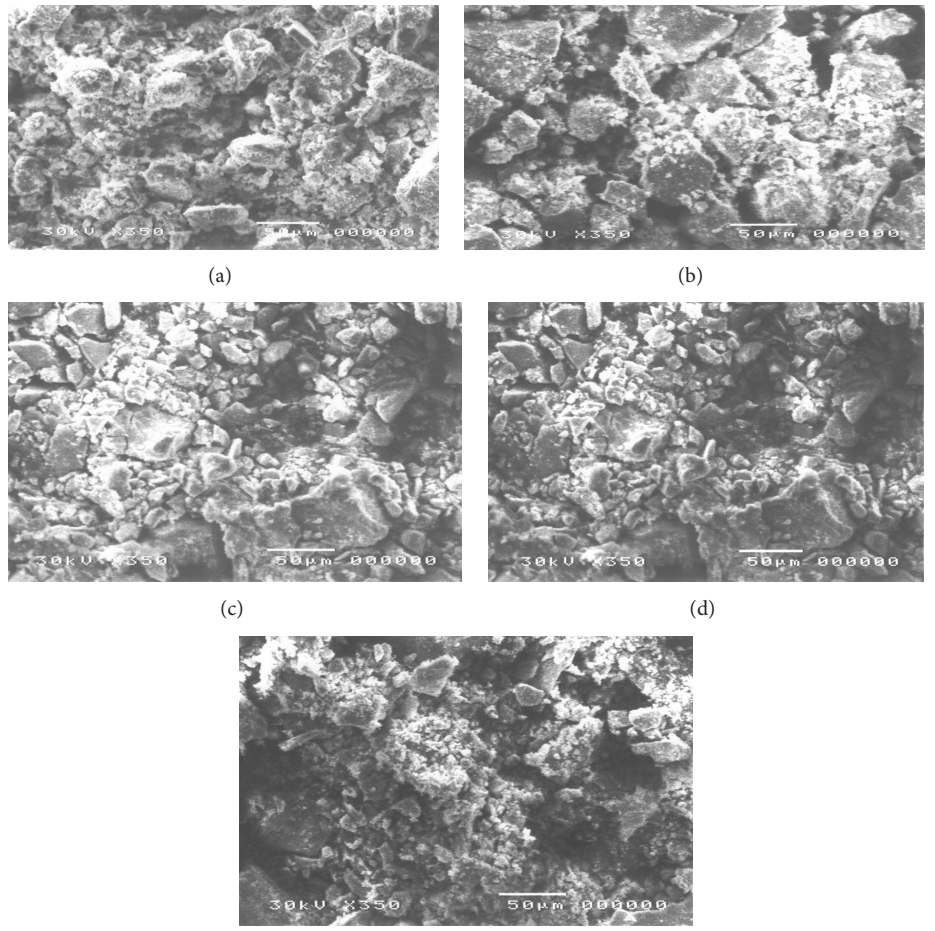

Figure 4: Scanning electron micrographs of irradiated samples (a) control, (b) 25 kGy, (c) 50 kGy, (d) 100 kGy, and (e) 150 kgy. All images were visible with aid of magnifying glass.

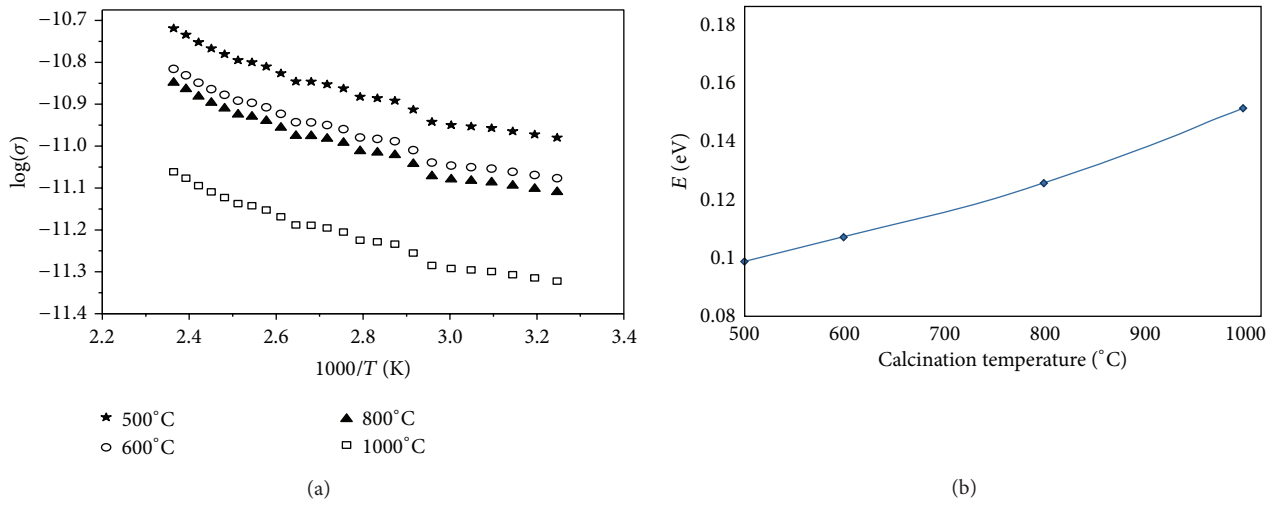

Figure 5: (a) Effect of sintering temperature on the electrical conductivity of ZnO/TiO_2 system calcined at different temperatures. (b) Effect of sintering temperature on the activation energy of electrical conductivity of ZnO/TiO_2 system calcined at different temperatures.

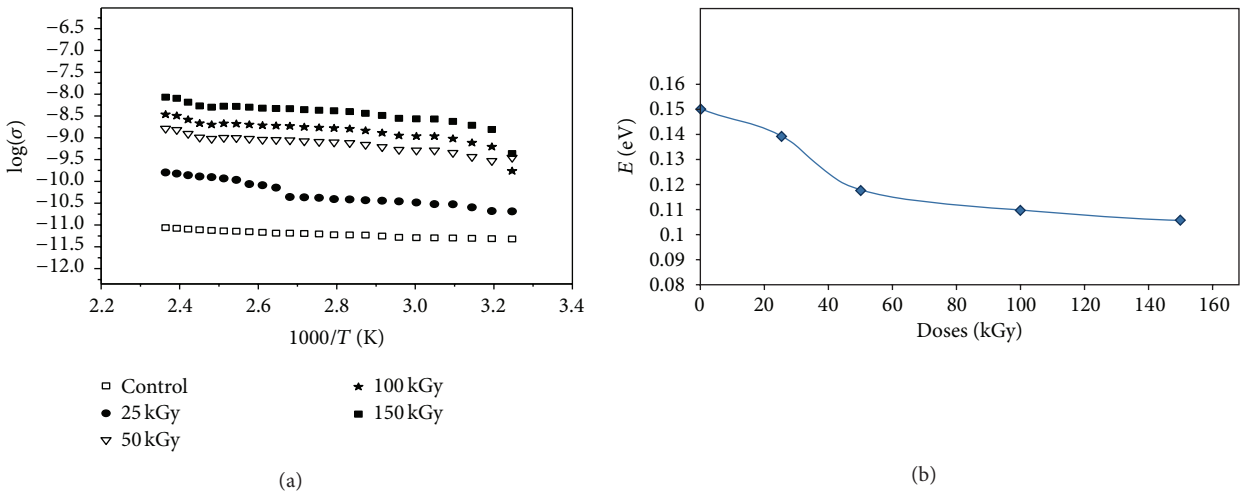

FIGURE 6: (a) Relationship between log σ and $1/T$ for ZnO/TiO_2 calcined at 1000°C and exposed to different doses of γ rays. (b) Effect of γ-rays doses on the activation energy of the electrical conductivity of ZnO/TiO_2 system calcined at 1000°C.

(1) Heating ZnO/TiO_2 system, prepared by sol-gel at 500–900°C, turned to $ZnTiO_3$-rohom and TiO_2-rutile.

(2) The produced phases existed as nano solids.

(3) The degree of crystallinity and crystallite size of $ZnTiO_3$-rohom and TiO_2-rutile increased by increasing the calcination temperature within 500–800°C.

(4) Increasing the calcination temperature of the system investigated up to 1000°C converted $ZnTiO_3$ from rohom structure to cubic phase together with a thermally stable TiO_2-rutile. The outstanding thermal stability of the rutile phase up to 1000°C has been attributed to a possible dissolution of some ZnO in the lattice of TiO_2-rutile forming solid solution.

(5) Gamma irradiation of the system investigated calcined at 1000°C decreased considerably the crystallite size of $ZnTiO_3$-cubic from 101 to 39 nm and that of rutile phase from 146 to 63 nm.

(6) Gamma irradiation increased considerably the electrical conductivity of irradiated solids with subsequent decrease in the activation energy of electrical conductivity.

Conflict of Interests

The authors declare that there is no conflict of interests regarding the publication of this paper.

References

[1] F. H. Dulin and D. E. Rase, "Phase equilibria in the system ZnO-TiO_2," *Journal of the American Ceramic Society*, vol. 43, pp. 125–131, 1960.

[2] S. F. Bartram and R. A. Slepetys, "Compound formation and crystal structure in the system ZnO-TiO_2," *Journal of the American Ceramic Society*, vol. 44, pp. 493–498, 1961.

[3] O. Yamaguchi, M. Morimi, H. Kawabata, and K. Shimizu, "Formation and Transformation of $ZnTiO_3$," *Journal of the American Ceramic Society*, vol. 70, no. 5, pp. 97–98, 1987.

[4] A. Baumgarte and R. Blachnik, "Isothermal sections in the systems $ZnOAO_2Nb_2O_5$ (A Ti, Zr, Sn) at 1473 K," *Journal of Alloys and Compounds*, vol. 210, no. 1-2, pp. 75–81, 1994.

[5] U. Steinike and B. Wallis, "Formation and structure of Ti-Zn-oxides," *Crystal Research and Technology*, vol. 32, no. 1, pp. 187–193, 1997.

[6] K. H. Yoon, J. Cho, and D. H. Kang, "Physical and photo-electrochemical properties of the TiO_2-ZnO system," *Materials Research Bulletin*, vol. 34, no. 9, pp. 1451–1461, 1999.

[7] R. Laishram, O. P. Thakur, D. K. Bhattacharya, and Harsh, "Dielectric and piezoelectric properties of la doped lead zinc niobate-lead zirconium titanate ceramics prepared from mechano-chemically activated powders," *Materials Science and Engineering B*, vol. 172, no. 2, pp. 172–176, 2010.

[8] W. Tai, "Photoelectrochemical properties of ruthenium dye-sensitized nanocrystalline SnO_2 :TiO_2 solar cells," *Solar Energy Materials and Solar Cells*, vol. 76, no. 1, pp. 65–73, 2003.

[9] S. A. El All and G. A. El-Shobaky, "Structural and electrical properties of γ-irradiated TiO_2/Al_2O_3 composite prepared by sol-gel method," *Journal of Alloys and Compounds*, vol. 479, no. 1-2, pp. 91–96, 2009.

[10] R. Kant, K. Singh, and O. P. Pandey, "Structural and ionic conductive properties of $Bi_4V_{2-x}Ti_xO_{11-\delta}(0 \le x \le 0.4)$ compound," *Materials Science and Engineering: B*, vol. 158, pp. 63–68, 2009.

[11] L. Khemakhem, A. Maalej, A. Kabadou, A. Ben Salah, A. Simon, and M. Maglione, "Dielectric ferroelectric and piezoelectric properties of $BaTi_{0.975}(Zn_{1/3}Nb_{2/3})_{0.025}O_3$ ceramic," *Journal of Alloys and Compounds*, vol. 452, no. 2, pp. 441–445, 2008.

[12] Y. Ku, Y.-H. Huang, and Y.-C. Chou, "Preparation and characterization of ZnO/TiO_2 for the photocatalytic reduction of Cr(VI) in aqueous solution," *Journal of Molecular Catalysis A: Chemical*, vol. 342-343, pp. 18–22, 2011.

[13] E. Yun, J. W. Jung, and B. C. Lee, "Effects of O_2 fraction on the properties of Al-doped ZnO thin films treated by high-energy electron beam irradiation," *Journal of Alloys and Compounds*, vol. 496, no. 1-2, pp. 543–547, 2010.

[14] K. G. Chandrappa and T. V. Venkatesha, "Generation of Co_3O_4 microparticles by solution combustion method and its Zn-Co_3O_4 composite thin films for corrosion protection," *Journal of Alloys and Compounds*, vol. 542, pp. 68–77, 2012.

[15] Y.-S. Chang, Y.-H. Chang, I.-G. Chen, G.-J. Chen, and Y.-L. Chai, "Synthesis and characterization of zinc titanate nanocrystal powders by sol-gel technique," *Journal of Crystal Growth*, vol. 243, no. 2, pp. 319–326, 2002.

[16] H. T. Kim, S. Nahm, J. D. Byun, and Y. Kim, "Low-fired (Zn,Mg)TiO_3 microwave dielectrics," *Journal of the American Ceramic Society*, vol. 82, no. 12, pp. 3476–3480, 1999.

[17] H. Obayashi, Y. Sakurai, and T. Gejo, "Perovskite-type oxides as ethanol sensors," *Journal of Solid State Chemistry*, vol. 17, no. 3, pp. 299–303, 1976.

[18] B. D. Cullity, *Publishing Cos*, pp. 102–105, Addison-Wesley, Reading, Mass, USA, 2nd edition, 1978.

[19] X. H. Zeng, Y. Y. Liu, X. Y. Wang, W. C. Yin, L. Wang, and H. Guo, "Preparation of nanocrystalline $PbTiO_3$ by accelerated sol-gel process," *Materials Chemistry and Physics*, vol. 77, no. 1, pp. 209–214, 2003.

[20] X. W. Wang, Z. Y. Zhang, and S. X. Zhou, "Preparation of nanocrystalline $SrTiO_3$ powder in sol-gel process," *Materials Science and Engineering B*, vol. 86, no. 1, pp. 29–33, 2001.

[21] Z. Surowiak, M. F. Kupriyanov, and D. Czekaj, "Properties of nanocrystalline ferroelectric PZT ceramics," *Journal of the European Ceramic Society*, vol. 21, no. 10-11, pp. 1377–1381, 2001.

[22] H. Fan and H. Kim, "Microstructure and electrical properties of sol-gel derived $Pb(Mg_{1/3}Nb_{2/3})_{0.7}Ti_{0.3}O_3$ thin films with single perovskite phase," *Japanese Journal of Applied Physics*, vol. 41, pp. 6768–6772, 2002.

[23] Y. S. Chang, I. G. Chen, and G. J. Chen, "Synthesis and characterization of zinc titanate doped with magnesium," *Solid State Communications*, vol. 128, no. 5, pp. 203–208, 2003.

[24] N. Obradović, N. Labus, T. Srećković, D. Minić, and M. M. Ristić, "Synthesis and characterization of zinc titanate nanocrystal powders obtained by mechanical activation," *Science of Sintering*, vol. 37, no. 2, pp. 123–129, 2005.

[25] H. T. Kim, Y. H. Kim, and J. D. Byun, "Phase transformation and thermal stability in zinc magnesium titanates," *Journal of the Korean Physical Society*, vol. 32, no. 1, pp. S159–S161, 1998.

[26] H. T. Kim, Y. H. Kim, and J. D. Byun, "Microwave dielectric properties of magnesium modified zinc titanates," *Journal of the Korean Physical Society*, vol. 32, no. 1, pp. 346–348, 1998.

[27] A. Golovchansky, H. T. Kim, and Y. Kim, "Zinc titanates dielectric ceramics prepared by sol-gel process," *Journal of the Korean Physical Society*, vol. 32, no. 3, pp. S1167–S1169, 1998.

[28] H. T. Kim, J. D. Byun, and Y. Kim, "Microstructure and microwave dielectric properties of modified zinc titanates (I)," *Materials Research Bulletin*, vol. 33, no. 6, pp. 963–973, 1998.

[29] L. M. Wang, "Applications of advanced electron microscopy techniques to the studies of radiation effects in ceramic materials," *Nuclear Instruments and Methods in Physics Research B: Beam Interactions with Materials and Atoms*, vol. 141, no. 1–4, pp. 312–325, 1998.

[30] O. M. Hemeda and M. El-Saadawy, "Effect of gamma irradiation on the structural properties and diffusion coefficient in Co-Zn ferrite," *Journal of Magnetism and Magnetic Materials*, vol. 256, no. 1–3, pp. 63–68, 2003.

[31] G. A. El-Shobaky, A. M. El-Shabiny, A. A. Ramadan, and A. M. Dessouki, "Effect of gamma irradiation on microstrain and lattice parameter of Co_3 O_4 loaded on Al_2 O_3," *Radiation Physics and Chemistry*, vol. 30, no. 4, pp. 233–236, 1987.